Asymptotic behavior of viscous-fingering patterns in circular geometry

David Jasnow and Chuck Yeung*
Department of Physics and Astronomy, University of Pittsburgh, Pittsburgh, Pennsylvania 15260
(Received 10 August 1992)

An examination of the scaling structure along with some extensive simulations on viscous fingering in circular geometry strongly suggest that the asymptotic patterns are compact. Experiments and simulations are in a transient regime that may exhibit a reasonable range where apparent fractal growth may be found. Arguments to connect the case of viscous fingering with that of vanishing surface tension are made.

PACS number(s): 47.20.−k, 47.55.Kf, 47.55.Mh, 68.10.−m

I. INTRODUCTION

When a less viscous fluid (say air) displaces a more viscous fluid (say water) between the closely spaced plates of a Hele-Shaw cell [1] in circular geometry, one might guess that the pattern defined by the fluid-fluid interface which ensues should be fractal. On large length scales one has a "Laplacian problem" with the inherent screening effects and, much like the case of diffusion-limited aggregation (DLA) [2], deep valleys might be left behind leading to a fractal structure (different in appearance from ordinary DLA, however). In circular geometry there may be no walls which, in rectangular geometry, can aid in producing regular shapes for the interface.

Unfortunately, the situation, both experimental and theoretical, has been somewhat equivocal. Ben-Jacob and co-workers [3, 4] advanced the notion of a dense-branching morphology for describing a wide class of growth processes in radial geometry (where tip splitting must take place). In this morphology a many-fingered configuration is enclosed by a compact, approximately circular envelope. Such structures have been observed in electrochemical deposition when the conductivity contrast is low [5, 6] or when diffusive effects are important [7, 8].

However, the situation for flow in a circular Hele-Shaw cell has been troubling. Available experimental evidence [9–11] and existing numerical solutions [12] have indicated that the patterns which develop in a circular Hele-Shaw cell, as a constant flux of a less viscous fluid displaces a more viscous one, are fractal with dimension approximately that of diffusion-limited aggregation [2] clusters (DLA), $D \sim 1.7$. Experiments by Couder [13], and numerical simulations by Sander, Ramanial, and Ben-Jacob [14], while not under constant-flux operating conditions, indicate similar results. But Ben-Jacob and co-workers and Buka and co-workers [15, 16] found that radial Hele-Shaw patterns did have the characteristic compact structure. Perhaps additional confusion was provided by Yeung and Jasnow [17], who reconsidered the quasilinear analysis of flow in circular Hele-Shaw geometry advanced in Refs. [3, 4]. They showed that, in contrast to the constant-pressure case, at constant flux there is no indication of a changeover to a compact structure. Furthermore, they suggested that the crossover in the case of constant pressure may be due to boundary conditions, namely a finite-size effect.

Some recent ideas on dimensional analysis contained in a primitive coarse graining-rescaling of the equation of motion of interfaces [18] suggested a new look at flow in a circular Hele-Shaw cell under constant-flux conditions. Dimensional analysis offers a connection: if the asymptotic pattern is fractal, then the surface tension introduces, to borrow terminology from critical phenomena, anomalous dimension (see, e.g., [19, 20]). The scaling analysis leads naturally to a method, which can be generalized to a variety of other problems, for varying a parameter to help determine if the data reflect asymptotic behavior. Armed with these ideas, more extensive simulations can be brought to bear on the question of asymptotic behavior, and on the evidence for anomalous dimension. The conclusion, for which evidence is offered below, is that under constant-flux conditions, radial Hele-Shaw patterns are not asymptotically fractal. This does not preclude the possibility of a range of data (both experimental and numerical) which may exhibit effective fractal properties.

The remainder of this paper is set out as follows. In the next section we briefly review the defining equations for flow at constant flux and consider the consequences of the dimensional analysis. We then review the evidence provided by the present series of simulations in which the flux and scale of the initial condition are systematically varied.

II. VISCOUS FINGERING IN CIRCULAR GEOMETRY

The defining equations for flow in circular Hele-Shaw geometry (see, e.g., [12]) are

$$\begin{aligned} \mathbf{V} &= -M\nabla P, \\ P|_I &= -d_0\mathcal{K}, \\ \int_I \mathbf{V}\cdot\hat{\mathbf{n}}d^{d-1}S &= Q, \end{aligned} \tag{2.1}$$

where d is the dimension of the bulk fluids and where we

have assumed, for simplicity, that the *displacing* fluid is inviscid. The subscript I indicates the limiting value at the interface from the viscous-fluid side. Here we have taken the pressure to be dimensionless, so that d_0, which is proportional to the surface tension, is a "microscopic" capillary length, and $\mathcal{K}$ is the curvature. The flux Q is constant in these operating conditions, and M denotes the mobility, depending, in the usual fashion, on the displaced liquid's viscosity and the spacing between the parallel plates (see, e.g., [12]). We supplement these equations by a length R_0 indicating the scale of the initial condition.

We now look at the consequences of dimensional analysis; the description in terms of dimensionless functions and variables is equivalent to the primitive coarse-graining, rescaling approach introduced by Jasnow and Viñals [18], and previous analysis by Sarkar [12, 21]. Introducing scales (P_0, T_0, L_0) for the pressure, time, and length, one finds that the defining equations become

$$\begin{aligned} \mathbf{v} &= -\nabla p, \\ p|_I &= -\kappa, \\ \int_I \mathbf{v}\cdot\hat{\mathbf{n}} d^{d-1}s &= 1, \end{aligned} \tag{2.2}$$

where now $p = P/P_0$ and $v = V/V_0 = VT_0/L_0$ are the reduced values, and κ is the reduced curvature. We have chosen the scale parameters to be $L_0 = (d_0M/Q)^{1/(3-d)}$, $P_0 = (Q/M)L_0^{2-d}$, $T_0 = L_0^d/Q$. Note that Eqs. (2.2) are parameter-free; hence, as pointed out previously [12], the interface equation describing the quasistatic evolution of the fluid-fluid boundary also contains no parameters. The consequences are that there may be a dependence on the initial conditions and that, in a regime in which the effect of the initial conditions is negligible, different physical realizations of the flows may be scaled into one another by adjusting the scales P_0, T_0, and L_0. In what follows we specialize to the physical case $d = 2$.

We imagine a set of initial conditions, Γ, specified by a length, R_0. To make contact with the numerical results to be presented, Γ can be thought of as circles of radius R_0, slightly perturbed by an assortment of Fourier modes such that the entire initial pattern has fourfold symmetry. Any characteristic length, $R(t)$, such as the radius of gyration of the pattern, averaged over the set of initial conditions, Γ, may now be expressed as L_0 times a function of the only two dimensionless ratios, $(t/T_0, R_0/L_0)$, i.e.,

$$R(t) = L_0F_2(t/(L_0^2/Q); R_0/L_0), \tag{2.3}$$

where $F_2(x;y)$ is a dimensionless function of its arguments. It should be recalled that R_0 sets the scale of the initial condition, so that $F_2(0;y) \sim y$. We first assume that the scale of the initial condition does not affect the asymptotic value of $R(t)$, and we will examine this assumption below. For now suffice it to say that for fixed "microscopic" parameters (Q, d_0, M), the radius of gyration empirically approaches a fixed curve, and the magnitude of R_0 affects a crossover time. Hence, asymptotically

$$R(t) = L_0F_1(Qt/L_0^2) = (Qt)^{1/2}F(L_0/(Qt)^{1/2}). \tag{2.4}$$

This final expression has a very suggestive form. Note that $(Qt)^{1/2} \equiv L(t)$ is a *macroscopic* length scale. The quantity $Qt = A(t) - A_0 = \Delta A$ is the incremental *area* of the pattern, which grows linearly in time in the constant-flux mode. The expression for $R(t)$ takes the asymptotic form

$$R(t) = L(t)F(L_0/L(t)) \simeq A^{1/2}f(L_0/A^{1/2}), \tag{2.5}$$

since, asymptotically, the initial area can be neglected.

Now, asymptotically, the macroscopic length $L(t) \to \infty$, so that $L_0/L(t) \to 0$. Recall that the *microscopic* length L_0 is proportional to d_0, which is itself proportional to the surface tension. From Eq. (2.5) one sees that in the growth kinetics the relative strength of the surface tension reduces to zero asymptotically as $t \to \infty$ [18], i.e., on the large scales. Stretching an analogy with critical phenomena, if there is no anomalous dimension, $F(x) \to F(0) = \text{const}$ as $x \to 0$, the pattern grows as $R \sim A^{1/2}$ and is not fractal. On the other hand if the limit is singular, namely

$$F(x) \sim x^{-\beta} \text{ as } x \to 0, \tag{2.6}$$

one finds a fractal structure with

$$\begin{aligned} R(t) &\sim f_sL_0^{-\beta}L(t)^{1+\beta} \\ &\sim f_s(d_0M/Q)^{-\beta}A^{1/D} \text{ with } D = 2/(1+\beta), \end{aligned} \tag{2.7}$$

where f_s is a dimensionless, universal constant, independent of system parameters. If $\beta \neq 0$ the relation of the linear size of the pattern to the area indicates a fractal structure, $A \sim R^D$; in that event note that the "anomalous exponent" β is accompanied by the singular dependence of the "critical amplitude" on the microscopic length $L_0 \propto d_0$.

In experiments noted above by Maher and co-workers [9–11], and previous simulations [12], the pattern for circular viscous fingering in the constant-flux mode appeared to be fractal with $\beta \sim 0.11$–0.18, which translates to $R \sim A^{1/D}$, with $D = 1.7$–1.8. However, the dynamic range of the experimental and numerical data is limited, and for limited data, a dimension in the above range is extremely difficult to distinguish from the compact $D = d = 2$. Here more extensive numerical solutions are reported which focus on the dependence of the critical amplitude and on the full scaling structure just described. As argued above, assuming no R_0 dependence, a fractal structure goes hand-in-hand with a singular dependence on the variable d_0/MQ. For technical reasons, it is difficult to vary d_0; hence the flux is varied with the initial scale of the pattern R_0 held fixed [22]. This is accomplished by writing $Q = qQ_0$, where Q_0 is a reference flux that determines scale parameters as $L_0 = (d_0M/Q_0)$, etc. Then the last line of Eq. (2.2) is replaced by

$$\int_I \mathbf{v}\cdot\hat{\mathbf{n}} ds = q, \tag{2.8}$$

where q is a dimensionless relative flux. Fractal growth will be indicated by the appearance of singular q dependence of the characteristic size of the structure, say, the

radius of gyration, according to

$$\tilde{R} \approx f_s q^{\beta} \tilde{A}^{1/D}. \tag{2.9}$$

Here the tildes (subsequently dropped) are used to indicate dimensionless numbers arising from a solution of the dimensionless equations (2.2) with the replacement (2.8).

Before turning to the numerical analysis, we consider again the scaling description, specifically the limit of vanishing surface tension. Intuitively one expects DLA-like behavior in this limit [1, 23], and it is useful to see the implications on the scaling structure. Reintroducing the dependence on the scale of the initial condition R_0, dimensional analysis requires

$$R = (\Delta A)^{1/2} f(L_0/(\Delta A)^{1/2}; R_0/L_0), \tag{2.10}$$

where again $L_0 = d_0 M/Q$ is proportional to the surface tension. This suggests that to study the $L_0 = 0$ limit (vanishing surface tension), one must find a different scaling, in which L_0 is eliminated. The effect is that the scale of the initial condition, R_0, can never be removed. (Another example of this feature is discussed in Refs. [20, 24].) One expects in this limit

$$\lim_{L_0 \to 0} f(x; y) = g(xy) = g(R_0/(\Delta A)^{1/2}). \tag{2.11}$$

Furthermore, one would expect that as its argument vanishes, i.e., for large scales, $g(z) \sim g_0 z^{-\beta'}$, where β' is the appropriate DLA-like exponent corresponding to $D \cong 1.7$. The strict limit $d_0 = 0$ may yield a different anomalous dimension from the possibility previously discussed, so we allow $\beta' \neq \beta$. We will return to a discussion of the full scaling function in two variables, Eq. (2.10), after presenting the numerical results.

III. NUMERICAL RESULTS

Numerical simulations have been carried out using the boundary integral equation described by Sarkar and Jasnow [12] with various code improvements developed by Viñals and Jasnow (see, e.g., [25]). The initial conditions for the simulations involve (unless otherwise stated) a circle of radius R_0 with a small perturbation involving a random distribution of eight modes in a quadrant. The entire perturbation is periodically continued into the other quadrants. A sample of the patterns that evolve is shown in Fig. 1.

First one must consider if, as discussed above, there are signs of an asymptotic region in which the effect of the initial conditions has been eliminated. In Fig. 2 we show, for fixed $q = 1$, the behavior of the radius of gyration, R_G, for several scales of initial conditions. Dividing by $A^{1/2}$ amplifies differences. The data indicate that, except for the largest initial condition, $R_0 = 1000$, which is not quite there yet, asymptotic behavior independent of initial conditions is setting in toward the end of the runs. To avoid cluttering the graph, one run for each initial scale has been shown; as will be seen, differences in initial conditions for the same (q, R_0) are quickly washed out.

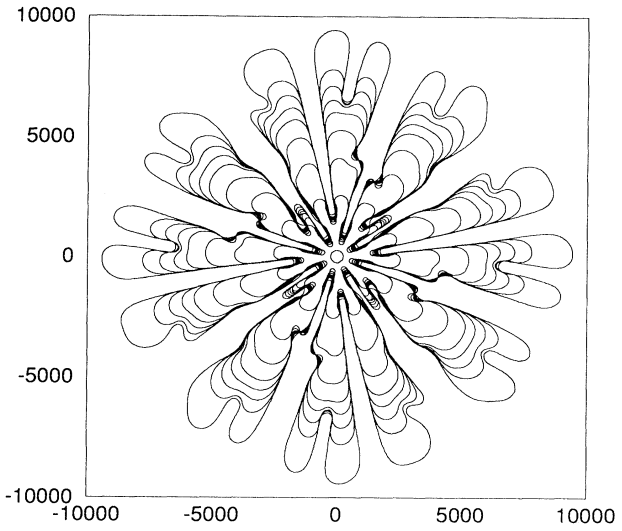

FIG. 1. Sample Hele-Shaw fourfold symmetric pattern produced for the case $R_0 = 250, q = 1$. The small "circle" is the initial condition. The curves are not equally spaced in time.

We note that the data even in these extensive simulations will permit a reasonable fit to $R_G \sim A^{0.55}$ over two decades of area variation. In Fig. 3 three runs with $(q = 1, R_0 = 500)$ are accumulated, showing the fit corresponding to $D = 1.82$.

In Fig. 4 a set of flux values $(q = 0.5, 1, 2, 4)$ with random initial conditions all having the same scale, $R_0 = 500$, are considered. According to Eqs. (2.7) and (2.9), in fractal growth, the "critical amplitude" depends on L_0, and the curves with successive q values should be offset from one another. Using the estimate $\beta = 0.14$, corresponding to $D = 1.75$ in the middle of the range of fractal dimension suggested by experiments and earlier simulations, yields the "error bar" in Fig. 4. Successive

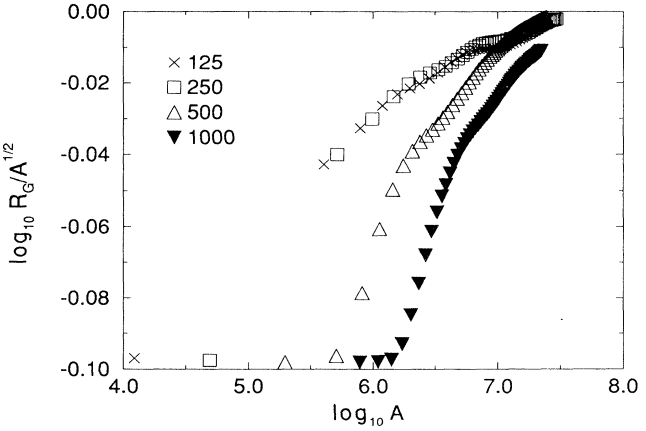

FIG. 2. Several runs with $q = 1$ and different scales of initial conditions showing that an asymptotic region of growth independent of initial conditions is setting in. The symbol labels correspond to values of R_0.

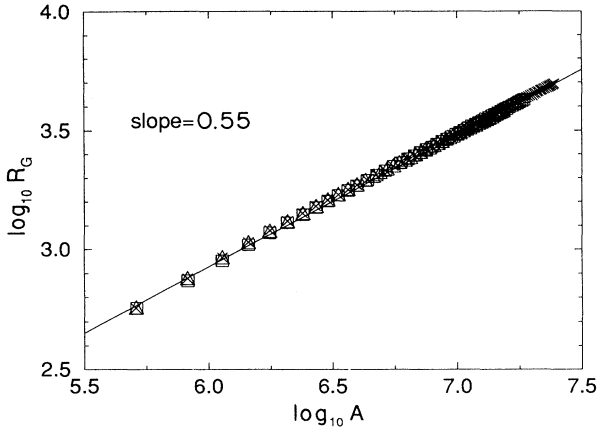

FIG. 3. Accumulated data for three runs with ($q = 1, R_0 = 500$) showing that over a substantial range, apparent fractal behavior describes the data. The slope of the line is 0.55 corresponding to a dimension $D \cong 1.82$, in the range of previous simulations and experiments.

curves for values of q differing by a factor of two should be offset by that amount. One sees that, if the data are approaching straight lines, the offset is likely to be less than that, suggesting that $\beta = 0.14$ is not the asymptotic value but rather is an overestimate. If the curves for different q values approach one another and a horizontal asymptote, it would be consistent with $\beta = 0$, indicating a compact structure. Note that different realizations for the same (q, R_0) fall closer together than curves for differing q.

We look more closely, now, whether even these extended simulations are truly asymptotic and whether the fractal dimension $D = 1.7$–1.8 extracted from experimental and numerical log-log plots is representing asymptotic data. If we assume the initial condition is irrelevant in the asymptotic behavior, it follows from Eq. (2.5) that in the asymptotic region, *irrespective* of whether or not the patterns are fractal, one must have $R(t)/A^{1/2}$ as a universal function of $Q\,A^{1/2}$, for fixed d_0 and M. By varying the relative flux q the asymptotics can be tested. The experiments of Maher and co-workers did include a range of flux values, but the overall precision available made it difficult to pin down the exponent. In Fig. 5 the approach to asymptotic behavior is examined for the same series of relative values of the driving flux ($q = 0.5, 1, 2, 4$). All the curves should coincide if the data are asymptotic. Clearly only the latest time data are beginning to show signs of collapse. If the merging curves are slowly diverging to infinity as $A \to \infty$, the structure is fractal. If, however, they are approaching a constant, the structure is compact with $D = d = 2$. Two straight lines for the asymptotic behavior are shown as a guide. The slope of the collapsed data yields the exponent β. The steeper straight line corresponds to $\beta = 0.14$, or $D = 1.75$, while the shallower line corresponds to $\beta = 0.03$ or $D = 1.94$. To obtain the larger slope, regions in which the data clearly do not collapse, i.e., are not asymptotic, must be included. Even with these more extensive simulations, only for a small region at the end are there signs of asymptotic behavior. Even if the combined curves are asymptotically diverging, assuming the final trend continues, the fractal dimension will be so close to $D = d = 2$ that it would be difficult for a laboratory experiment or a simulation to distinguish the structure from a compact one. However, there is the possibility that there are oscillations and that the collapsed data will systematically diverge as $qA^{1/2}$ is increased, with a power more like $\beta = 0.14$. We will return to this possibility below.

A method to consider the trends in a more quantitative manner is to look at the "effective exponent" defined by

$$D_{\text{eff}}^{-1} = \frac{d\log_{10}(R_G)}{d\log_{10}(A)} = (1 + \beta_{\text{eff}})/2. \tag{3.1}$$

We show in Fig. 6 effective exponents for $q = 1$ with several scales for the initial conditions [26]. The oscil-

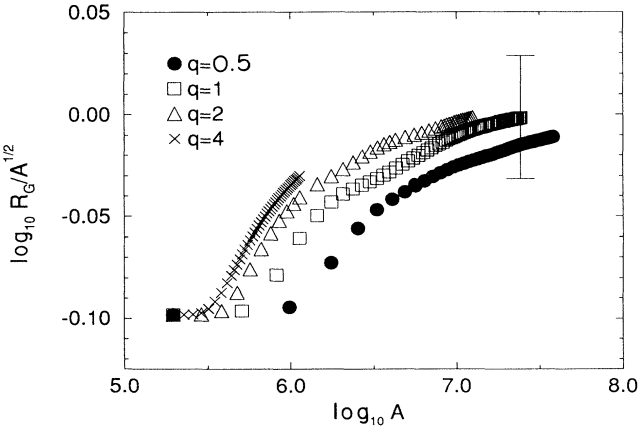

FIG. 4. Runs for different relative flux values with initial condition characterized by $R_0 = 500$. This shows that the data for different q values appear to be converging. For asymptotic fractal behavior one expects successive curves to be separated by the amount indicated in the error bar.

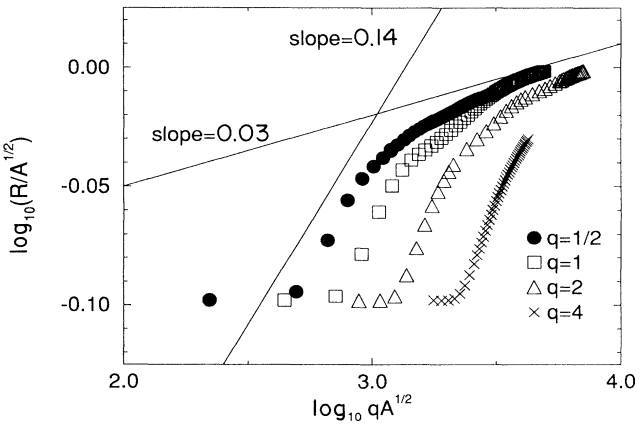

FIG. 5. Scaled data indicating the beginnings of asymptotic collapse. The slope corresponds to the anomalous exponent β. The different relative flux values are indicated, and for all runs $R_0 = 500$.

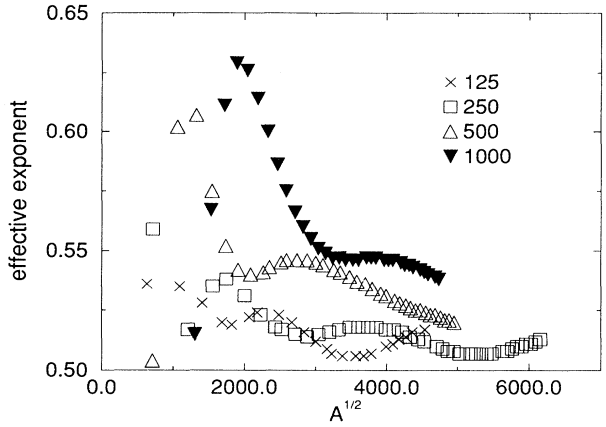

FIG. 6. Effective exponent for several runs with $q = 1$. The symbols label the scale of the initial condition, R_0. The effective exponent is an estimate of the inverse of the fractal dimension, D^{-1}.

lations are seen as is the trend toward lower values of β_{eff} as the scale of the initial condition is decreased. For Fig. 7 four extended runs corresponding to different initial conditions with $q = 1, R_0 = 125$ were performed. The oscillations tend to occur at different places (reflecting the specific initial condition) and averaged data are smoother. Figure 7 indicates a trend to small and possibly vanishing values of β.

IV. CONCLUDING REMARKS

While we cannot rule out asymptotic fractal growth with an exponent much closer to $D = d = 2$ than previously suggested, our conclusion is that for flow at constant flux in circular geometry, the structures which evolve are not asymptotically fractal. Notice once again in Fig. 1 that some attempts at tip splitting are annealed, and if that trend continues, the pattern will not become more complex. The surface tension, while controlling

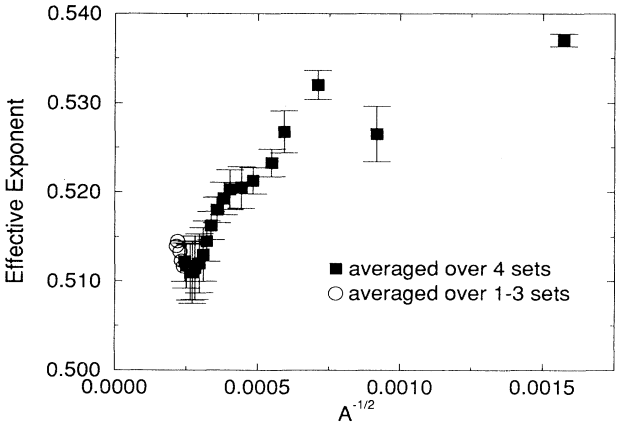

FIG. 7. Effective exponent for four extensive runs with $q = 1, R_0 = 125$, showing the average and the spread of the data.

bends in the interface only on the smallest length scales, makes itself felt on the largest scales and, in spite of the screening inherent in Laplacian problems, prevents fractal structure. In the language of critical phenomena, the surface tension does not appear to introduce anomalous dimension. For fixed d_0 and $A^{1/2} \to \infty$ the scaling function goes smoothly to a constant.

Some interesting features and possibilities are worthy of additional consideration. First, the simulations for individual runs give clear indication of the oscillations predicted by Sarkar [27] in a mean-field theory of the tip-splitting cascade. This makes determinations from limited data exceptionally difficult. Sarkar's theory, while representing an important advance, is, unfortunately, not parameter free and is not inconsistent with asymptotically compact viscous-fingering patterns. A very interesting question arises as to the nature of the crossover, since apparently experiments and any future simulations are surely to lie in the crossover regime. One may ask whether it is possible to have an asymptotically compact structure and yet an infinite range of fractal behavior. If there are only a finite number of decades of apparent fractal behavior, then an entire experiment can be considered to be in a transient regime. Heuristic arguments suggest a transient regime of approximate DLA-like behavior which gets wider the smaller one makes $L_0 \sim d_0$.

To see this, consider again the full scaling in the form of Eq. (2.10). Based on the numerical simulations and other arguments given above, the scaling function must satisfy

$$f(x;y) \to \begin{cases} f_0 \text{ for fixed } \infty > y > 0 \text{ as } x \to 0, & (4.1) \\ g_0(xy)^{-\beta'} \text{ as } y \to \infty,\ xy \to 0, & (4.2) \\ g_2 xy \text{ with } xy \to \infty, & (4.3) \end{cases}$$

where f_0, g_0, and g_2 are constants. The first line embodies asymptotic compactness; the second line produces genuine fractal behavior (at large enough area) for zero surface tension; the third line says that at early time $\Delta A \to 0$ and R must be on the order of R_0. An approximant which satisfies all the requirements is of the form

$$f(x;y) = h(x)\left[g_0^{-1}(xy)^{\beta'} + f_0^{-1}\right]^{-1} + g_2 xy[1-h(x)], \tag{4.4}$$

where $h(x)$ is a smooth crossover function going from unity for $x \ll x_1 = O(1)$ to zero for $x \gg x_1$. This will reproduce qualitatively the shape seen in Fig. 4, but with $\beta = 0$, i.e., with the curves asymptotically flattening out. A small finite $\beta \neq 0$ could easily be incorporated. A range of DLA-like behavior characterized by anomalous exponent β' will exist for $x_1 \gg x \gg (g_0/f_0)^{1/\beta}/y$. The larger $y = R_0/L_0$ is, the wider is the apparent fractal range. In the limit $L_0 \to 0$, the range can be infinite. Recalling that $y \gg 1$ for small d_0 (surface tension) or at large flux, Q, these arguments suggest that only in the limit of vanishing surface tension (or infinite flux) will the fractal range be infinite. A crossover from fractal to

compact structure in terms of viscosity contrast has been discussed by Lee, Coniglio, and Stanley [28].

We have been imagining that the scaling function $f(x;y)$ describes the average over a set of initial conditions; accordingly the average may wash out the oscillations predicted by Sarkar [27]. Within the basic dimensional analysis, an analogous scaling can be presented for a single run, but additional dimensionless parameters are needed to specify the initial condition. Sarkar [29] has recently performed an interesting analysis of the fractal regime making detailed comparisons between numerical calculations and laboratory experiments to, among other things, test the adequacy of the modeling.

Comments on the other common operating condition, *constant pressure*, are in order. A new length R_1 enters the problem, representing the outer ring with fixed pressure (atmospheric, in a laboratory experiment). The equations cannot be made parameter-free in that case [12,17]. Only in an intermediate regime, when the radius of gyration is much greater than the initial condition but much smaller than the outer ring, can the structure be fractal. But when the outer ring size does not matter, there should not be a material difference between constant pressure and constant flux. It is therefore likely that patterns under constant pressure are fractal only in an intermediate regime, but the evolution to a compact shape (in any reasonable experiment) may be interfered with by the presence of the outer boundaries.

Reanalysis of the nature of the scaling of viscous fingering in a circular Hele-Shaw cell combined with additional simulations at constant flux thus strongly suggests that the growth patterns are not asymptotically fractal [30]. There is not much in the way of intuitive understanding of this result as it has been previously shown [17] that the quasilinear analysis of Refs. [3,4] are inconclusive. This "simplest" of all pattern forming systems remains intriguing. Additional understanding can perhaps be obtained via a suitable modification of Sarkar's [27] mean-field theory of the tip-splitting hierarchy.

Finally we note that this approach of carefully examining the implications of dimensional analysis to determine if data are asymptotic can be applied to a variety of related problems which are expected to yield power-law growth. An interesting example is that of spinodal decomposition in which case the analog of R_0 could be the correlation length of the initial state.

ACKNOWLEDGMENTS

We would like to thank Dr. Timothy Rogers for his substantial efforts in behalf of this work, particularly in the development of the computer code, and also Mr. Junichi Iwasaki for his assistance. We thank Dr. Knut Jørgen Måløy for his interest and helpful discussions. The support of the NSF under Grant No. DMR89-14621 is gratefully acknowledged. We thank the Pittsburgh Supercomputing Center, where the bulk of the computations were performed, and the SCRI, Florida State University, where several computer-memory-intensive runs were carried out with the help of Dr. Jorge Viñals.

* Present address: Department of Physics, University of Toronto, Toronto, Ontario, Canada M5S 1A7.

[1] For a review of viscous flow in two dimensions, see, e.g., D. Bensimon, L. P. Kadanoff, S. Liang, B. I. Shraiman, and C. Tang, Rev. Mod. Phys. **58**, 977 (1986).
[2] T. A. Witten and L. M. Sander, Phys. Rev. Lett. **47**, 1400 (1981).
[3] E. Ben-Jacob, G. Deutscher, P. Garik, N. D. Goldenfeld, and Y. Lareah, Phys. Rev. Lett. **57**, 1903 (1986).
[4] E. Ben-Jacob, P. Garick, and D. Grier, Superlatt. Microstruct. **3**, 599 (1987).
[5] S. Sawada, Physica A **140**, 134 (1986).
[6] Y. Sawada, A. Dougherty, and J. P. Gollub, Phys. Rev. Lett. **56**, 1260 (1986).
[7] G. Deutcher and Y. Yareah, Phys. Rev. Lett. **60**, 1510 (1988).
[8] S. Alexander, R. Bruinsma, R. Hilfer, G. Deutcher, and Y. Yareah, Phys. Rev. Lett. **60**, 1510 (1988).
[9] S. N. Rauseo, J. P. D. Barnes, and J. Maher, Phys. Rev. A **35**, 1245 (1987).
[10] M. W. DiFrancesco, S. N. Rauseo, and J. V. Maher, Superlatt. Microstruct. **3**, 617 (1987).
[11] S. E. May and J. V. Maher, Phys. Rev. A **40**, 1726 (1989).
[12] S. K. Sarkar and D. Jasnow, Phys. Rev. A **39**, 5299 (1989).
[13] Y. Couder, in *Random Fluctuations and Pattern Growth*, edited by H. E. Stanley and N. Ostrowsky (Kluwer Academic, Dordrecht, 1988) .
[14] L. M. Sander, P. Ramanial, and E. Ben-Jacob, Phys. Rev. A **32**, 3160 (1985).
[15] A. Buka and P. Palffy-Muhoray, Phys. Rev. A **36**, 1527 (1987).
[16] A. Buka, P. Palffy-Muhoray, and Z. Racz, Phys. Rev. A **36**, 3984 (1987).
[17] C. Yeung and D. Jasnow, Phys. Rev. A **41**, 891 (1990).
[18] D. Jasnow and J. Viñals, Phys. Rev. A **41**, 6910 (1990).
[19] D. J. Amit, *Field Theory, the Renormalization Group, and Critical Phenomena* (McGraw-Hill, New York, 1978).
[20] N. D. Goldenfeld, O. Martin, Y. Oono, and F. Liu, Phys. Rev. Lett. **64**, 1361 (1990).
[21] S. K. Sarkar, Superlatt. Microstruct. **3**, 589 (1987).
[22] The node spacing in any numerical solution may impose an effective surface tension which is difficult to control since the number of nodes is dynamically adjusted. For this reason it is preferred to vary the relative flux.
[23] P. Meakin, F. Family, and T. Vicsek, J. Colloid Interface Sci. **117**, 394 (1987).
[24] L.-Y. Chen, N. Goldenfeld, and Y. Oono, Phys. Rev. A **44**, 6544 (1991).
[25] J. Viñals and D. Jasnow, in *Computer Simulations in Condensed Matter*, edited by D. P. Landau, K. K. Mon, and H. B. Schutter (Springer-Verlag, Berlin, 1992) .
[26] In numerically differentiating the log-log data, we consider pairs of points separated by a factor of two in area. This eliminates detailed structure over a small fraction of a decade.

[27] S. K. Sarkar, Phys. Rev. Lett. **65**, 2680 (1990).
[28] J. Lee, A. Coniglio, and H. E. Stanley, Phys. Rev. A **41**, 4589 (1990).
[29] S. K. Sarkar (unpublished).
[30] It is unlikely that the present numerical calculations can be pushed significantly further without major modifications. For increased computational efficiency in extremely long runs, more care has to be exercised in the dynamical distribution of nodes describing the interface.